Combined effects of Ga, N, and Al codoping in solution grown 3C–SiC

J. W. Sun, G. Zoulis, J. C. Lorenzzi, N. Jegenyes, H. Peyre, S. Juillaguet, V. Souliere, F. Milesi, G. Ferro, and J. Camassel

Citation: Journal of Applied Physics **108**, 013503 (2010); doi: 10.1063/1.3455999
View online: http://dx.doi.org/10.1063/1.3455999
View Table of Contents: http://scitation.aip.org/content/aip/journal/jap/108/1?ver=pdfcov
Published by the AIP Publishing

Combined effects of Ga, N, and Al codoping in solution grown 3C–SiC

J. W. Sun,[1] G. Zoulis,[1] J. C. Lorenzzi,[2] N. Jegenyes,[2] H. Peyre,[1] S. Juillaguet,[1] V. Souliere,[2] F. Milesi,[3] G. Ferro,[2] and J. Camassel[1,a)]
[1]*Groupe d'Etude des Semiconducteurs, UMR 5650, CNRS, Université Montpellier 2, cc 074-GES, 34095 Montpellier Cedex 5, France*
[2]*Laboratoire des Multimateriaux et Interfaces, UMR 5615, CNRS, UCB-Lyon1, 43 Bd du 11 nov. 1918, 69622 Villeurbanne, France*
[3]*CEA-LETI/MINATEC, DPTS/SLIDE, 17 rue des Martyrs, 38054 Grenoble Cedex 9, France*

(Received 16 April 2010; accepted 20 May 2010; published online 1 July 2010)

We report on Ga-doped 3C–SiC epitaxial layers grown on on-axis (0001) 6H–SiC substrates using the vapor-liquid-solid technique and different $Si_{1-x}Ga_x$ melts. The resulting samples have been investigated using secondary ion mass spectroscopy (SIMS), micro-Raman spectroscopy (μ-R) and, finally, low temperature photoluminescence (LTPL) spectroscopy. From SIMS measurements we find Ga concentrations in the range of 10^{18} cm^{-3}, systematically accompanied by high nitrogen content. In good agreement with these findings, the μ-R spectra show that the Ga-doped samples are *n*-type, with electron concentrations close to 2×10^{18} cm^{-3}. As expected, the LTPL spectra are dominated by strong N–Ga donor-acceptor pair (DAP) transitions. In one sample, a weak additional N–Al DAP recombination spectrum is also observed, showing the possibility to have accidental codoping with Ga and Al simultaneously. This was confirmed on a non-intentionally doped 3C–SiC (witness) sample on which, apart of the usual N and Al bound exciton lines, a small feature resolved at 2.35 eV comings from neutral Ga bound excitons. Quantitative analyses of the DAP transition energies in the Ga-doped and witness sample gave 346 meV for the optical binding energy of Ga acceptors in 3C–SiC against 251 meV for the Al one. The conditions for the relative observation of Ga and Al related LTPL features are discussed and the demonstration of room temperature luminescence using Ga doping is done. © *2010 American Institute of Physics*. [doi:10.1063/1.3455999]

I. INTRODUCTION

For many years, promising technological applications for high power and high temperature electronic devices have made silicon carbide (SiC) an important semiconductor material.[1] SiC crystallizes in many different forms (polytypes) and, among the large variety of SiC polytypes, 4H–SiC is the most advanced one in terms of device development.[2] However, due to the cubic ZnS-type structure and lower band gap energy, 3C–SiC keeps specific interest.[3] First is a lower interface trap density at the SiC/SiO_2 interface and, second, better understood transport properties. Unfortunately, despite decades of 3C–SiC material studies and growth technology development, the progress in electronic device performances is low. In the case of 3C–SiC, and for a long time, it has been hampered by the lack of large single crystal substrates, resulting in poor quality of the active epitaxial layers. This is no longer true.

Recently, the growth of cubic SiC on thick (bulklike) free standing epitaxial layers,[3] complemented by the growth on hexagonal substrates by the vapor-liquid-solid (so-called VLS) technique,[4,5] allowed improvement of the crystal quality of the cubic structures. This opened the way for new device developments, like improved MOS structures[3,6] or lightly doped *p-n* junctions with innovative junction termination extension (JTE).[7] To speed up the process, still remains the crucial issue of reproducibly growing (and nondestructively evaluating) high quality epitaxial material. This is well mastered for *n*-type doping but, for *p*-type material, the situation is entirely different.

Basically in SiC and whatever the polytype, all group III substitutional impurities (like B, Al, Ga, or In) are potential *p*-type doping species. Indium has a too low solubility limit at usual growth temperatures[8] and can be easily discarded. Remain only B, Al, and Ga. Among them aluminum, which is isochoric to Si, gives the shallowest acceptor level for all SiC polytypes.[9] This is the basic reason why it has been most investigated. Concerning only 3C–SiC, Zanmarchi[10] reported in 1968 the observation of an orange photoluminescence band at 77 K in crystals grown by the van Harkel method in a gaseous mixture of Si, C, and Al chlorides. Two years later, Choyke and Patrick[11] reported additional observations of the same luminescence band now identified as coming from neighboring N–Al donor-acceptor pairs (DAP) spectra-in Lely-grown 3C–SiC crystals. Similar spectra were later observed in Al-doped 3C–SiC films grown by chemical vapor deposition (CVD) on Si substrates by Freitas *et al.*[12] and, from these observations, the presence of Al acceptors in 3C–SiC with optical binding energy ~250 meV above the maximum of the valence band is a well established result.[9] This primary set of investigations was complemented by Clemen *et al.*[13] who reported in the early 1990s on the radiative recombination of excitons bound to isolated (neutral) Al ac-

a)Electronic mail: jean.camassel@ges.univ-montp2.fr

TABLE I. VLS Growth conditions and SIMS results obtained for the average values of Ga, N, and Al concentrations in the Ga-doped 3C–SiC samples investigated in this work.

Sample	Melt composition	Growth conditions (°C/min)	Thickness (μm)	Growth rate (μm/min)	[Ga] ($\times 10^{18}$ cm^{-3})	[N] ($\times 10^{19}$ cm^{-3})	[Al] ($\times 10^{15}$ cm^{-3})
A	$Si_{0.25}Ga_{0.75}$	1200/30	1.3	0.04	3.87	3.34	~3
B	$Si_{0.1}Ga_{0.9}$	1050/30	0.3	0.01	9.69	7.65	~0.9
C	$Si_{0.5}Ga_{0.5}$	1300/10	1.9	0.19	3.24	4.53	~3

ceptors. From these crossed examinations, the nondestructive (optical) evaluation of N and Al impurity contents in 3C–SiC is no longer a problem.[14]

Since aluminum can cause problems when processing devices (because it can form clusters after high dose ion-implantation[15] and/or has a high affinity to oxygen[16]), Kuwabara *et al.*[17,18] reported also on Ga and B incorporation. From different spectra collected on Ga- and B-doped samples, they deduced optical ionization energies of ~343 meV for Ga (Refs. 9 and 17) and 735 meV for B.[18] Such "optical" ionization energies do not change much through the all family of SiC polytypes[9] and, comparing with aluminum, this makes boron an alternative (deeper) acceptor that can be used to get low doped JTEs. Combined with nitrogen and activated by optical pumping, it can also participate in the constitution of an efficient light-emitting medium for white light-emitting diode (LED) applications.[19] A strong drawback is that most of the technological applications request ion-implantation technology, while annealing B species is not so well mastered.[20,21]

Much less is known concerning gallium. There are only few reports in the literature, Ref. 22–25, and apart from the works of Refs. 17 and 25 all focus on the hexagonal (6H or 4H) polytypes. This includes the work of Ref. 22 in which, from "sandwich" sublimation epitaxy, the solubility limit on the {0001} plane in 6H–SiC was found to be 1.2×10^{19} cm^{-3} at 2000 °C or the work of Ref. 23 in which, from transport experiments, the ionization energy of Ga acceptors was found at 290 meV and 300 meV from the topmost valence band in 6H and 4H–SiC, respectively. This includes also the works of Refs. 23 and 24 in which deep level transient spectroscopy was done on CVD grown and implanted 4H and 6H–SiC. The only exception is the work of Ref. 25 in which the recombination spectra of Ga-bound excitons was identified in all three polytypes. Strictly speaking, even if the usual behavior of acceptor impurities is close in the different polytypes there has ***never*** been any electrical investigation of the incorporation and activation of Ga species in 3C–SiC. As a consequence, from the literature data, nobody can really tell whether the Ga acceptor binding energy becomes shallower with increasing Ga concentration (as suggested in the work of Ref. 23) or not. Becoming shallower, it would follow the behavior of Al and B acceptors and allow some reasonable *p*-type doping. Staying constant, it would not and the final doping level would be very sensitive to compensation. This lack of knowledge has several consequences. Except the works of Refs. 22–24, no real effort has been done to investigate Ga doping as a possible alternative to Al doping in microelectronics or to measure the solubility limit in 3C epitaxial layers or to identify the residual Ga compensation (if any) in low doped *n*-type material. Even more, the possibility of accidental (or intentional) Ga and Al codoping has never been envisaged.

In this work, we demonstrate that Ga can be introduced in solution grown 3C–SiC up to a maximum value of ~3 to 4×10^{19} cm^{-3} at growth temperature ranging from 1050 to 1300 °C. Then, because of the rather low value of the solubility limit at growth conditions used in this work we demonstrate that, when accidental codoping by N species happens, it can easily compensate the material. It becomes *n*-type, without any possibility to investigate directly (from Hall-effect measurements) the electrical ionization energy of Ga acceptors in 3C–SiC. Only remains the optical techniques and "optical binding energy" (346 meV) that can be deduced from the consideration of DAP spectra. Finally, and because accidental codoping with Al often happens in nonintentionally doped material, we investigate the combined effects of N, Al, and Ga codoping.

II. EXPERIMENTAL DETAILS

Three different 3C–SiC layers grown on the Si-face of on-axis (0001) 6H–SiC substrates have been considered. We used the standard VLS technique and, to modify the Ga concentration, tuned simultaneously the growth temperature and the Si/Ga ratio. For sample A we used a $Si_{0.25}Ga_{0.75}$ melt fed with 5 SCCM (SCCM denotes cubic centimeter per minute at STP) propane for 30 min at 1200 °C. For sample B we used a $Si_{0.1}Ga_{0.9}$ melt and, to reduce Ga evaporation, the growth temperature was reduced to 1050 °C for 30 min. Finally, for sample C a $Si_{0.5}Ga_{0.5}$ melt was used at growth temperature 1300 °C for 10 min. The thickness of the samples was deduced from infrared reflectivity measurements (not shown) and the results listed in Table I. They show that the reduction in growth temperature reduces the growth rate from about 0.2 to 0.01 μm/min per minute.

For comparison, a nonintentionally doped 3C–SiC layer (sample D) was also used. It was homoepitaxially grown by CVD at 1500 °C on top of a 3C–SiC layer grown by VLS. For the VLS layer a $Si_{0.25}Ge_{0.75}$ melt was used fed with 3 SCCM propane in two steps. A first step was done at 1450 °C for 5 min and, next, a final step at 1200 °C for 60 min. This VLS template, with thickness 1.8 μm, was then thickened to ~6 μm by CVD at 1500 °C using SiH_4 and C_3H_8 diluted in H_2. The corresponding C/Si ratio in the gas phase was 3.

Secondary ion mass spectroscopy (SIMS) measurements were done on the Ga-doped VLS samples to control the

amount of incorporated impurities. We used a modified Cameca IMS 4*f* equipment with an O^{2+} ion source. The primary beam voltage was 15 kV and the primary current about 650 nA. This resulted in an average etching rate of ~25 Å/s. To calibrate the concentration, implanted reference samples were used. For gallium, for instance, the implantation energy of $^{69}Ga^{+}$ ions was 225 keV and the dose 1×10^{14} cm^{-2}. Of course, depending on the impurity and acquisition conditions the detection limit (DL) varied. It was $\sim10^{14}$ cm^{-3} for Ga (with a similar value for Al) but remained relatively high ($\sim10^{17}$ cm^{-3}) for N with a large dependence on acquisition conditions (mainly vacuum pumping level).

To control activation, micro-Raman (μ-R) spectra were collected at room temperature using the 633-nm line of an He–Ne laser as excitation wavelength. A confocal configuration was used but, even using a microscope to increase the spatial resolution down to few micrometer square, the contribution coming from the 6H–SiC substrate could not be fully eliminated.

Finally, low temperature photoluminescence (LTPL) spectra were collected at 5 K using a frequency doubled Ar^{+}-ion laser for excitation ($\lambda=244$ nm). The nominal (incident) power was ~30 mW and a Jobin Yvon-Horiba Triax 550 spectrometer, fitted with a 600 g/mm grating and a cooled charge coupled device camera, completed the setup.

III. RESULTS AND DISCUSSION

A. SIMS and (μ-R) spectroscopy

Depth profiles of the Ga and N concentrations are shown in Fig. 1. A first point to notice is that, every time, for the three Ga-doped samples the highest Ga concentration is found at the epilayer to substrate interface. In other words, the Ga concentration increases when moving from the surface to the interface. This behavior is not new and similar to the one already noticed in the case of Al-incorporation during VLS growth in Al–Si melts.[26] Of course, since the concentration is not homogeneous, we only list the average values in Table I.

A second (interesting) feature appears when considering the peak values noticed for the Ga concentration at the substrate to epilayer interface. In all three samples we find very similar values (see Fig. 1) varying only from 3 to 4 $\times10^{19}$ cm^{-3}. We believe that this value corresponds to the effective Ga solubility limit (SL) in 3C–SiC at growth conditions used in this work. We do not know whether or not it depends on the incorporation of additional impurities like nitrogen (see below) but it is lower by, at least, one order of magnitude with respect to the one previously reported for Al in 3C–SiC using a similar growth procedure.[26] It is also ~6 times higher than the result of theoretical predictions from Ref. 8. Hopefully, it is in reasonable agreement with the experimental value ($\sim1.2\times10^{19}$ cm^{-3}) reported by Vodakov *et al.*[22] in 6H–SiC at sublimation temperature ~1800 K. Most probably the difference between the two experimental results comes from the difference in growth techniques, rather than the difference in grown polytypes. This is the basic reason why a liquid phase process is often preferred to reach a high doping level.

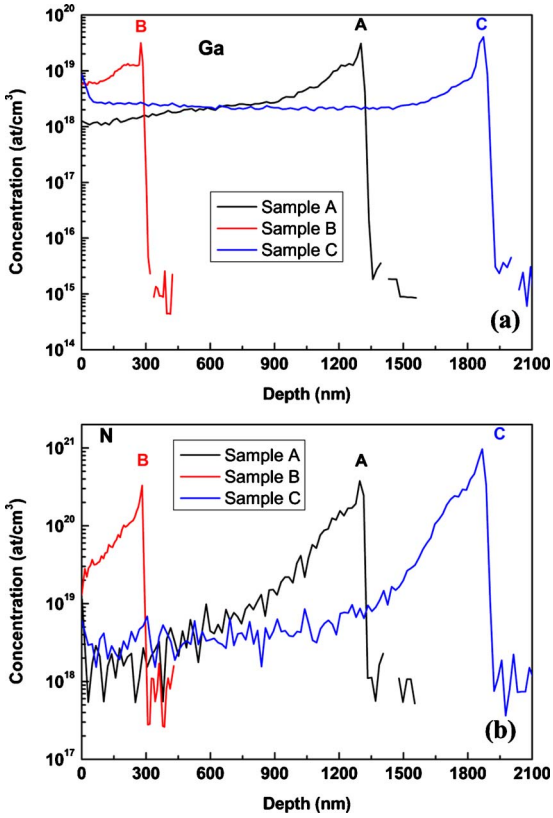

FIG. 1. (Color online) Calibrated SIMS measurements of (a) the Ga and (b) the N concentration in the three Ga-doped 3C–SiC samples investigated in this work. The zero (starting point) is always located at the surface of epilayers.

As already said, apart of the low (effective) SL, a most surprising result is the high level of nitrogen coincorporation. It is at least similar, and most of the time higher than the Ga one. Moreover, the N content follows regularly the Ga one (or vice versa). A clear example is the N and Ga profiles collected for sample C in the near surface region. The Ga concentration first decreases and then increases. The N profile does exactly the same, which suggests that some interaction does exist between the two elements during the VLS growth. This point is still under investigation and, even, the nitrogen origin (which is inherent to the growth set-up used in this work) is not perfectly clear. In some cases, it could be eliminated.[27] In most cases it cannot and additional work has to be done to clarify the incorporation mechanism. At the present time, the only clear point is that the coincorporation of N and Ga atoms at such elevated concentrations should result in strongly compensated material, with poor electrical properties or even (from Table I) with final *n*-type carrier concentration. This is exactly what is found.

In Fig. 2 we show μ-R spectra collected at room temperature on, both, the Ga-doped samples and a control piece of bare 6H–SiC substrate. Consider, first, Fig. 2(a). For clarity all experimental spectra have been shifted vertically, with maximum intensity normalized to unity. Since the penetration depth of the 633 nm laser line is larger than the thickness of the 3C–SiC deposit,[28] a strong signal coming from the 6H–SiC substrate is observed. A good example is the peak at ~796 cm^{-1} which corresponds with zone-center TO-

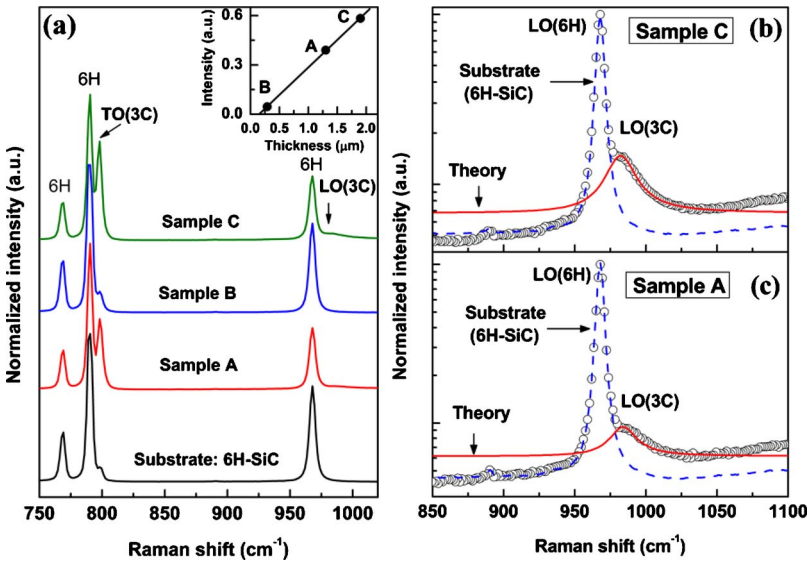

FIG. 2. (Color online) (a) Comparison of room temperature Raman spectra collected on the three Ga-doped samples and a bare 6H–SiC substrate. For clarity, all spectra have been normalized and shifted vertically. The inset shows the change in intensity of the 796 cm^{-1} Raman mode (TO-3C) vs the 3C SiC film thickness; (b) and (c) comparison of experimental (empty circles) and calculated (full lines) line shapes for the LO-phonon plasmon coupled mode in samples A and C. The dashed curve shows the experimental LO phonon peak coming from the 6H–SiC substrate.

phonon modes in, both, 3C–SiC and 6H–SiC. In the backscattering configuration we used, the scattered light intensity should be high for 3C and weak for 6H.[29] In other words, adding a 3C epilayer on top of a 6H substrate should increase the signal intensity. This is exactly what is found. With respect to the naked (control) piece of sample, the scattered intensity increases when focusing on the top epitaxial layer which gives a clear evidence of a 3C–SiC deposit on top of the 6H–SiC substrates. Of course, in this case and for very thin samples, the extra intensity should be proportional to the thickness of the 3C–SiC layer. Again, this is exactly what is found. Within experimental uncertainty, the magnitude of the (extra) 3C–SiC signal scales directly like the thickness values listed in Table I. This is shown in the inset of Fig. 2(a).

Concerning more specifically the *n*-type doping suggested by the results of the SIMS experiments, let us consider more in details the μ-R spectra in the range 850–1100 cm^{-1}. Results for the thicker samples A and C are shown on an enlarged scale in Figs. 2(b) and 2(c), respectively. In both cases, we resolve two different LO-phonon frequencies with the sharper (stronger) modes coming now from the 6H–SiC substrates. The smaller (broader) ones come from the Ga-doped 3C–SiC layers. This is not found for sample B because of a too small epitaxial layer thickness and/or a too large phonon damping and, in this case, the 3C–SiC LO-mode is (almost completely) obscured by the signal coming from the 6H–SiC substrate. This was not the case for the thicker samples and, in both cases, the 3C LO frequency resolved at ~984 cm^{-1}, on the high energy side of the 6H–SiC mode. This is a well-known feature for all SiC polytypes[29,30] which comes when an over-damped plasmon couples with a LO-phonon mode. On a totally independent basis, this confirms the results of the SIMS measurements. In good agreement with the results of Table I, the two Ga-doped samples are not *p*-type but instead *n*-type.

More quantitative results can be found when fitting the shape of the LPP (LO-phonon plasmon) modes. We follow the path of Yugami *et al.*[30] and calculate the line shape for samples A and C with parameter values listed in Table II. The results are shown as solid lines in Figs. 2(b) and 2(c), respectively. The agreement is good and gives electronic concentrations $\sim 2\times 10^{18}$ cm^{-3} in both samples. The only difference between sample A and sample C is the carrier mobility. In sample A we find ~66 $cm^2\ V^{-1}\ s^{-1}$ and only ~48 $cm^2\ V^{-1}\ s^{-1}$ in sample C.

To compare these optical (electronic) concentrations with the SIMS results, a nondegenerate, single-donor/single-acceptor model has been used. For any partly compensated *n*-type material with $N_D > N_A > n$, the carrier concentration should be given by[31]

$$n = \left(\frac{N_D}{N_A} - 1\right)\frac{N_C}{g_D} e^{-E_D/k_B T}, \tag{1}$$

in which N_D and N_A are the donor and acceptor concentrations ; g_D is the donor degeneracy factor (g_D=2); E_D is the donor binding energy (with E_D=54 meV for nitrogen[12]); T is the absolute temperature, and k_B is the Boltzmann's constant. The effective conduction-band state density is taken as $N_C = 2(2\pi m^* k_B T)^{3/2} h^{-3}$, in which m^* is the electrons effective mass taken as[30] ($0.313 m_0$). To estimate N_D and N_A we used the SIMS concentrations listed in Table I and found for the net electron concentrations: $\sim 2.1\times 10^{18}$ cm^{-3} in sample A and 3.51×0^{18} cm^{-3} in sample C. This is in excellent agree-

TABLE II. Parameter values used to calculate the line shapes of the LO-phonon plasmon coupled modes in the Ga-doped 3C–SiC samples.

Sample	Plasmon frequency ω_p (cm^{-1})	Plasmon damping constant γ (cm^{-1})	Phonon damping constant Γ (cm^{-1})	Faust–Henry coefficient C	Electron concentration n (cm^{-3})	Mobility μ($cm^2\ V^{-1}\ s^{-1}$)
A	289	450	10	0.35	2×10^{18}	66
C	289	620	10	0.35	2×10^{18}	48

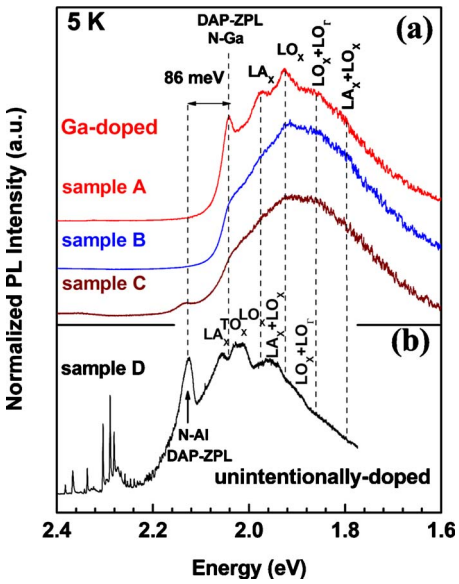

FIG. 3. (Color online) Comparison of LTPL spectra collected at 5 K on (a) three Ga-doped samples grown by VLS on a 6H–SiC substrate and (b) a nonintentionally doped CVD layer grown on top of a 3C–SiC VLS layer (see text).

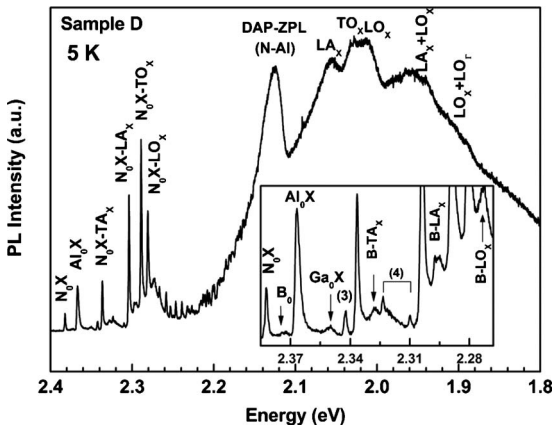

FIG. 4. High resolution LTPL spectrum collected at 5 K on the nonintentionally doped sample D. The inset shows an enlarged portion of the near band edge spectrum. The Ga_0X line corresponds to a four-particle Ga-bound exciton complex. The lines denoted by shell number (m) are due to discrete N–Al DAP transitions.

ment with the results obtained from the line shape analysis of the μ-R spectra.

To summarize this part, we have shown the following.

- When growing in the temperature range 1050–1300 °C, gallium can be introduced in solution grown 3C–SiC up to a maximum value (SL) of ~3 to 4×10^{19} cm^{-3}. This is typically one order of magnitude below the aluminum concentration that can be introduced in the same polytype when using the same technique;
- because of this low SL value, nitrogen codoping can easily be more important than gallium doping. This is the case in the series of samples investigated in this work;
- this makes them n-type, heavily Ga-compensated, without any possibility to investigate directly (from Hall effect measurements) the electrical properties and ionization energy of Ga acceptors in 3C–SiC;
- to some extent, this can be done from the consideration of DAP recombination spectra and we come now to the results of LTPL measurements.

B. LTPL results

In Fig. 3 we compare two different series of LTPL spectra. First, in Fig. 3(a) are the results collected for the Ga-doped samples (A, B, and C). Next, in Fig. 3(b) is a spectrum collected for the nonintentionally doped sample D. The vertical lines are guides for the eyes. They have been drawn to indicate the relative energy positions of the two different contributions. Let us, first, consider Fig. 3(a). Focusing on sample A we find an intense LTPL spectrum at 5 K, dominated by a strong recombination band at 2.039 eV and four phonon replicas. They come from one phonon (LA_X and LO_X) or two-phonon mode (LA_X+LO_Γ and LO_X+LO_Γ) contributions. This is very similar to the 20 K spectrum reported for Ga-doped 3C–SiC crystals by Kuwabara *et al.*[17] and, without any ambiguity, we assign the 2.039 eV band to the N–Ga DAP zero-phonon line (hereafter called DAP-ZPL). For samples B and C, the DAP spectra are not so well resolved but, still, similar features can be found. As already said, this difference in experimental resolution is not an accident. Most probably, it comes from the difference in total Ga and N-incorporation levels in the near surface region. Indeed, since the penetration depth[28] of the 244 nm laser line in 3C–SiC is less than ~500 nm, most of the observation field is limited to the near surface area where the first sample (A) has a lower (total) impurity concentration (including N and Ga) than samples B and C (see Fig. 1). This is why the carrier mobility is better in sample A than sample C (see Sec. III A) and why the experimental resolution of LTPL spectra is better in sample A than samples B and C.

A second interesting point to consider is that, despite poorer experimental resolution, we find a small (but specific) feature near 2.125 eV in sample C. It is located 86 meV away from the N–Ga DAP-ZPL and comes from the ZPL band of N–Al DAPs. This is obvious from the consideration of LTPL spectra collected on sample D [see Fig. 3(b)] and suggests a 86 meV binding energy difference.[32] While this is a first (direct) evidence of accidental Ga and Al codoping, this is ***not*** the only one. Consider more in details the LTPL spectra collected on sample D. They have been shown on an expended scale in Fig. 4 and evidence the following:

- due to the low level of residual doping in this (witness) sample, the near band edge (NBE) spectrum is dominated by a complex series of narrow NBE exciton lines. They did not resolve in the Ga-doped samples and come from a complex admixture of recombination lines coming from the annealing of one and two excitons bound to N or Al impurities with phonon replicas. For details, see Refs. 11, 13, 14, 33, and 34;
- among these sharp NBE exciton lines is a weak band, at about 2.35 eV, noticed Ga_0X in the inset of Fig. 4. It comes from the radiative recombination of excitons

bound to neutral Ga atoms[25] and, on a pure experimental basis, confirms that in both intentionally and nonintentionally Ga-doped samples gallium can accompany (or be accompanied by) aluminum as residual *p*-type impurities;

- this is true whatever the residual Al and Ga concentrations are. In sample C the Ga and N concentrations were $\sim 3.2\times10^{18}$ cm^{-3} and $\sim 4.5\times10^{19}$ cm^{-3}, respectively and, to obtain the (unknown) Al concentration, additional SIMS measurements were done. We found $\sim 3\times10^{15}$ cm^{-3} (see Table I). In sample D and, again, from SIMS measurements the Al and N concentrations were $\sim 2.2\times10^{16}$ cm^{-3} and 4.6×10^{17} cm^{-3}, respectively, while the Ga concentration remained below the SIMS detection limit. To get estimate one needs an optical calibration tool, similar to the one developed in the work of Ref. 14 for N and Al impurities ;
- we forget about everything else and, to estimate the Ga concentration in sample D, we write that the ratio of recombination line intensities for neutral Ga and Al bound excitons obeys the simple relationship[14]

$$\frac{I(Al_0X)}{I(Ga_0X)} = \frac{[Al]R^{\tau}(Al_0X)}{[Ga]R^{\tau}(Ga_0X)}. \quad (2)$$

In this expression, R^{τ} is the ratio of nonradiative $\tau^{nr}(i)$ and radiative $\tau^{r}(i)$ lifetimes of excitons bound to a neutral acceptor "i" (with i=Al,Ga). In the first approximation we suppose that, both, the radiative and nonradiative lifetimes are independent of the chemical nature of the impurity and the difference in core size. In this way, we get from the ratio of integrated lines intensity in Fig. 4 a concentration value $[Ga]\sim 2.3\times10^{15}$ cm^{-3} which is one order of magnitude higher than the SIMS DL. This is clearly wrong and shows that additional changes in lifetimes (either radiative or nonradiative or both) have to be taken into account. We shall come back to this point in the Sec. IV.

Let us first discuss the origin of the Ga impurities. At the present time, it is not clear to decide where these extra acceptor species are coming from. The VLS growth mechanism implies the contact of a graphite crucible with the melt[4] and Al is a well-known impurity in graphite with residual incorporation varying from run to run.[35] Since sample C was grown at higher temperature than samples A and B, this may explain why Al codoping was found in sample C and not in samples A and B. For sample D, grown by CVD at even higher temperature, but without any intentional doping, both Al and Ga impurities should also come from the graphite susceptor.

Whatever the origin, despite the coexistence of two different acceptors we notice that one single (broad) continuum of DAP transitions resolves in sample D with ZPL band centered at ~2.125 eV (see Fig. 4). It comes from the main N–Al DAP features, without any strong (easy to identify) N–Ga related ones. This is opposite to the experimental finding encountered in sample C (see Fig. 3) in which the ZPLs energy difference (86 meV) moved the high energy/low intensity Al-related features out of the low energy/high intensity (Ga-related) ones. This is the main reason why in sample C, and even with a low integrated intensity ratio of 1/42 between the N–Al and N–Ga DAP features, it could resolve so easily. In sample D this is not the case. The gallium contribution merges systematically with the N–Al phonon replicas (see vertical lines in Fig. 3) and there is no way to identify them rapidly. Only the strong N–Al features can be identified with, of course and depending on the relative level of Ga codoping, more or less interference with the hidden N–Ga contribution. This probably explains why, in many cases, the phonon energies deduced from the experimental lines position differ from the (expected) experimental values obtained for 3C–SiC at Γ and X-points of the Brillouin zone (see Refs. 10, 11, and 36).

To summarize, we have found evidence of simultaneous codoping with Al and Ga acceptors in two 3C–SiC samples (samples C and D) grown in two different reactors, using two different growth techniques. Such accidental codoping originates, most probably, from unknown graphite parts and should ***not*** be exceptional. Similar (accidental) codoping with Al and B has been already observed (at least for one sample) in the work of Ref. 19 and, to avoid long and destructive SIMS examinations, it looks appealing to use optical techniques to evaluate the relative acceptor concentrations.

IV. PROBING RELATIVE ACCEPTOR CONCENTRATIONS FROM OPTICAL STUDIES

We focus on the simple case in which only two different acceptor species (A_1 and A_2) are simultaneously present. To check if one can estimate their relative concentration from the ratio of related LTPL lines (integrated) intensities, we start from Eq. (2). From the Sec. III B we know that some changes in radiative and/or nonradiative lifetimes has to be taken into account. In such a case the ratio of radiative recombination lines for the excitons bound to a neutral acceptor $(A_0)_1$ or $(A_0)_2$ can be written

$$\frac{I(A_0X)_1}{I(A_0X)_2} = \frac{[A_1]R^{\tau}(A_0X)_1}{[A_2]R^{\tau}(A_0X)_2}. \quad (3)$$

From the experimental results collected on sample D (see Sec. III B) the change in radiative lifetimes is not small. Typically, to make the ratio of acceptor concentrations deduced from the SIMS measurements ($[Al]/[Ga]\sim 10^2$) in good agreement with the ratio of LTPL line intensities $[I(Al_0X)/I(Ga_0X)\sim 10]$ the ratio of radiative and nonradiative lifetimes must decrease by a factor of 10 when moving from Al to Ga.

For DAP spectra, the situation is similar. We know[14,19] that the radiative recombination intensity for a given DAP band is driven by the product of two terms. The first one is simply the product of the acceptor concentration $[A_i]$ times the probability for a hole in the valence band to trap at site A_i. We call it: $[h(A_i)]$. The second one is the ratio of nonradiative and radiative lifetimes for the bound electron-hole pair: $R^{\tau}(D\text{-}A_i)$. This gives

$$\frac{I_1(\text{D-A}_1)}{I_2(\text{D-A}_2)} = \frac{[\text{A}_1]R^{\tau}(\text{D-A}_1)}{[\text{A}_2]R^{\tau}(\text{D-A}_2)}. \quad (4)$$

As already said, the experimental situation for sample C is such that the Al contribution in Fig. 3 is ~42 times smaller than the Ga one. Assuming again a factor of 10 for the ratio of radiative and nonradiative lifetimes around both impurities, this gives an Al concentration of the order of 7.7×10^{15} cm^{-3}, in reasonable agreement than the one (3×10^{15} cm^{-3}) determined by SIMS (see again Table I).

Obviously, this is the large difference in core size that exists between Al (isochoric to Si) and Ga (isochoric to Ge) that influences the details of the radiative and nonradiative recombination processes. This is true for the excitons bound to a neutral acceptor atom (A_0X complex) and the DAP transitions. However, at the present time, it cannot be said whether this is an increase in radiative lifetime (coming from some neglected part of process like a lower trapping efficiency for holes or a lower electron-hole overlap) or a shorter nonradiative lifetime (induced by strain) or both that lowers the R ratio when moving from Al to Ga. To further analyze this point let us consider in detail the change in trapping efficiency.

A. Trapping efficiency at two different acceptor sites

In *n*-type materials, the radiative recombination rate for an exciton bound to a neutral donor atom (D_0X complex) is driven by the probability for the donor to trap an electron, then to bind a hole and, finally, to recombine radiatively. When the first term is the most limiting one,[37] one can apply the theory of Lax[38] which gives for the capture cross-section of an electron by a neutral donor

$$\sigma = \left(\frac{eh^2}{8m^*\varepsilon^2 E_b^3}\right)^{1/2}. \quad (5)$$

In this expression σ is the capture cross-section; m^* is the effective mass of electrons; ε is the dielectric constant, and E_b is the donor binding energy.

In partly compensated *n*-type materials (this work) there are, simultaneously, neutral donors bound excitons, neutral acceptors bound excitons (A_0X complex), and DAP transitions (DAP lines). For the A_0X complex, we follow the same path and assume that the radiative recombination rate of an exciton bound to a neutral acceptor is driven by the probability for the acceptor to trap a hole which, next, binds an electron which, finally, recombines. For the DAP transitions, we assume that the radiative recombination rate for an electron from the conduction band (or an electron trapped to a donor atom) to recombine with a hole bound to an acceptor is always driven by the probability for a hole to trap around an acceptor.

In both cases we assume that the limiting factor is the hole capture rate (whatever the details of the binding mechanism are) and express the capture cross-sections using Eq. (5). The binding energy depends on the chemical nature of the acceptor. It depends also on the mechanism under consideration. For a DAP transition, it is the usual hole binding energy. For an A_0X complex, it is the exciton binding energy. For usual SiC polytypes (including 3C) it is given by the Haynes rule[25]

$$E_b(A_0X)_i = -14.9 \text{ meV} + 0.16E_b(A)_i. \quad (6)$$

This shows that, whatever the mechanism under consideration, to take into account the specific nature of the acceptor it is necessary to determine E_b accurately.

B. Binding energies of Ga and Al acceptors

We start from DAP spectra in samples A and D and focus on the resolution of discrete pairs components. Taking into account this finite pair distance (r_{DA}) the emitted photon energy should be given by[39,40]

$$h\upsilon(r_{DA}) = E_g - (E_D + E_A) + \frac{e^2}{4\pi\varepsilon r_{DA}} - E_{vdW}. \quad (7)$$

In this expression, E_g is the band gap energy; E_D and E_A are the binding energy of the donor and acceptor A_i; e is the electronic charge, and ε is the static dielectric constant at liquid helium temperature (9.7 from the work of Ref. 11). The last term is a van der Waals (vdW) polarization term associated with the dipole–dipole interaction between the neutral donor and the neutral acceptor in the initial state of the pair transition. It is of the form

$$E_{vdW} = \frac{e^2}{4\pi\varepsilon R_{DA}}\left(\frac{b}{r_{DA}}\right)^5. \quad (8)$$

in which b is a constant, specific of donors D and acceptors A_i. Finally, for type II spectra, the relation between r_{DA} and m is given by

$$r_{DA} = (8m-5)^{1/2}a_0/4, \quad (9)$$

in which a_0=4.36 Å for 3C–SiC.

In the series samples investigated in this work, we could hardly find a LTPL spectrum with a complete (large) series of sharp (discrete) DAP lines coming from the close pair recombination spectrum. This is illustrated in Fig. 5 for Al and Ga, respectively. Consider, first, Figs. 5(a) and 5(b). Both refer to N–Al DAP recombination lines, in which the assignment of the shell number m is made from a fit of the line intensity distribution according to the expected values given by the number of equivalent lattice sites in a given shell.[11,17,39,40] A second guidance is provided by the shell substructure resolved for low shell numbers (see m=4,8). However, in some cases, this shell substructure is partly obscured by phonon replicas of a bound exciton complex. This is the case of shells m=6 and m=7 in Fig. 5(a). Altogether, this makes the assignment not straightforward. For N–Ga DAPs, the situation is even worse. In Fig. 5(c) for sample A, we could only resolve a discrete series of lines with shell number $m<12$ and, to increase accuracy, we had to complement our data with the results of Ref. 17.

The comparison with compulational results is shown in Fig. 6. The solid lines are obtained from Eq. (7) with and without vdW correction terms. For $r_{DA}>17$ Å ($m>30$) both curves are very similar and give an excellent fit to the experimental data. For $r_{DA}<17$ Å, this is no longer true and

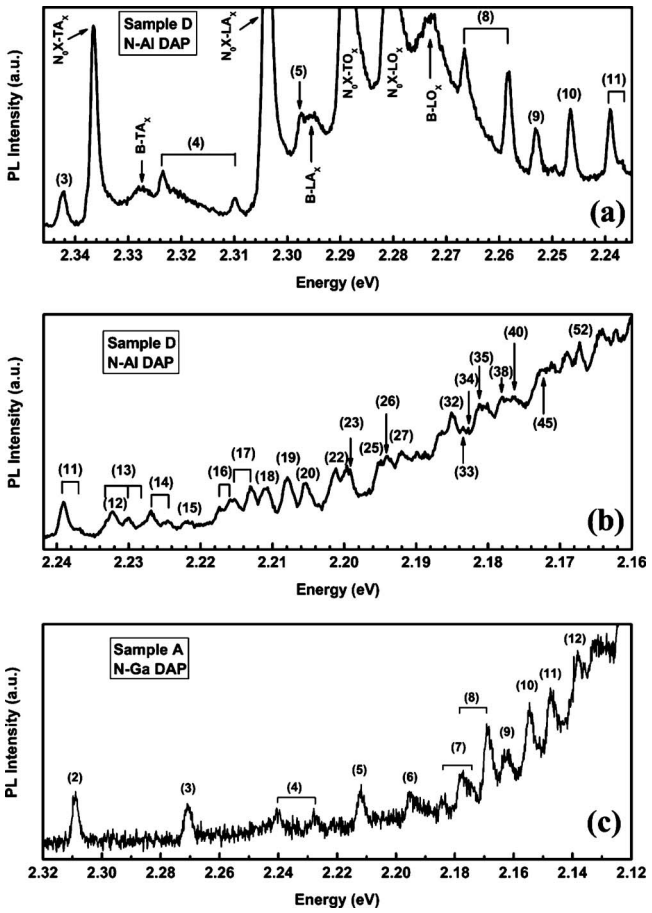

FIG. 5. Parts of LTPL spectra collected on samples D and C. For sample D, they show well-resolved discrete series of DAP lines coming from close N–Al pairs with (a) $m<11$ and (b) $m>11$. For sample A, discrete series of N–Ga DAP lines with $m<12$ are also found (c). The shell number values (m) are given between brackets.

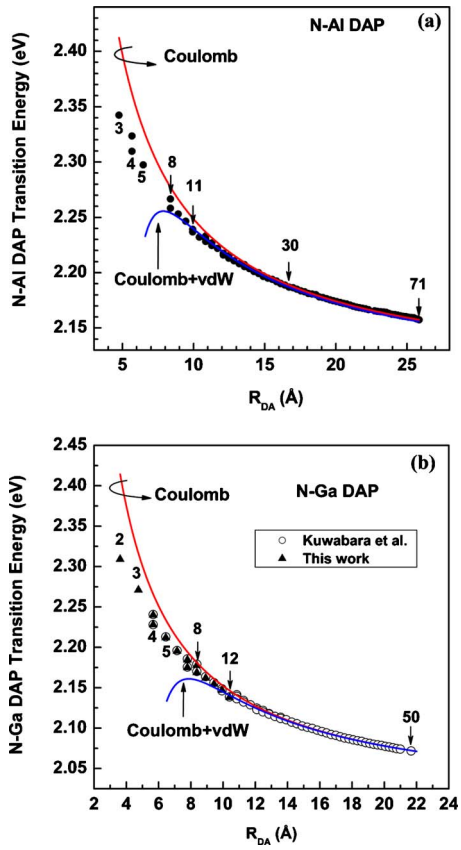

FIG. 6. (Color online) Fit of the transition energies computed for the N–Al (a) and N–Ga (b) discrete line spectra vs pair distance r_{DA}. For N–Ga, the triangles show the experimental results collected in this work, the open circles come from the work of Kuwabara *et al.* (Ref. 17). The solid curves follow Eq. (7) with and without van der Waals interaction.

the simple Coulomb terms (without E_{vdW}) deviate gradually from the experimental results in such a way that, for $m>8$ one needs to consider both the Coulomb and the vdW terms (taking a value $b=6$ Å for the effective vdW constant). Finally, for $m<8$ both curves deviate from the experimental results because the dielectric continuum formulas (7) and (8) become invalid when the DAP separation term becomes smaller than the sum of the ground-state radius of the donor and acceptor atoms.

From the best fits in Fig. 6 we find $h\upsilon(r_{DA}\rightarrow\infty)=2.099$ eV for the N–Al DAP lines and 2.004 eV for the N–Ga ones. Taking 2.390 eV for the excitonic energy gap in cubic SiC;[36] 13∼14 meV for the exciton binding energy[9] and 54 meV for the N donor binding energy[12] the Al and Ga acceptor binding energies come out to be: 251 meV and 346 meV, respectively. The energy difference (95 meV) appears in reasonable agreement with the 86 meV value estimated from the DAP spectra in Fig. 3 but, even correcting for the difference in capture cross-section, we cannot account for the difference in radiative recombination rates between Al and Ga. There must be some additional effect which comes from the neglected part of process. This can be either a lower electron-hole overlap for a given pair distance or a shorter nonradiative lifetime or both.

To summarize, up to now considering only the difference in binding energy (trapping efficiency) we have been unable to account for the difference in recombination rate between Al and Ga acceptors. Apart of the local strain (which comes from the difference in core size) there must be some additional effects (like central cell corrections) which increases the whole localization. In this case they should also lower the temperature dependence. This is checked in the Sec. V.

V. TEMPERATURE DEPENDENCE

In Al-doped SiC samples, the N–Al DAP luminescence spectrum often disappears around liquid nitrogen temperature. On the opposite, despite (or because of) a large optical binding energy (735 meV at liquid helium temperature) heavily boron-doped 6H–SiC has been recently recognized[19] as an efficient light emitting medium, working up to 250 K and suitable for white LED applications using optical pumping. From the intermediate binding energy obtained for Ga atoms, one would expect an intermediate behavior with a small temperature dependence of the overall intensity of the N–Ga DAP recombination spectrum.

To check this hypothesis, temperature-dependent investigations have been done on sample A. The results are shown in Fig. 7 in the temperature range 5–300 K. Clearly, when the temperature increases, the spectra become less and less resolved and the ZPL band gradually broadens. Up to 200 K,

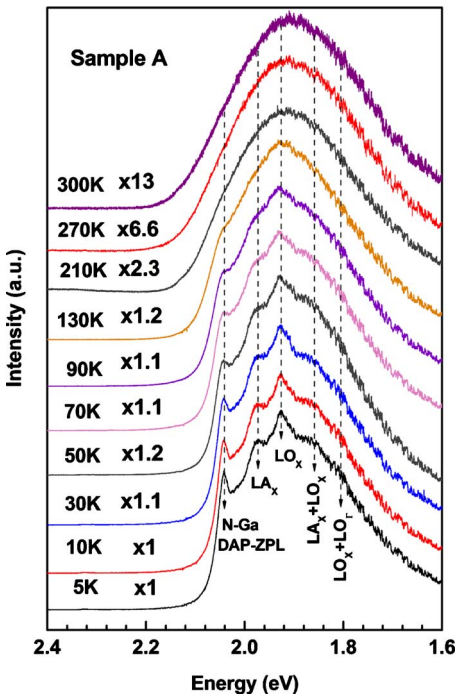

FIG. 7. (Color online) Temperature dependence of the PL spectra collected on sample A from 5 to 300 K.

the overall intensity is not much affected. Above 200 K, the N–Ga DAP-ZPL structure becomes weaker and broader in such a way that, at room temperature, one cannot identify the DAP-ZPL fine feature of and phonon replicas anymore.

From this temperature dependence it is obvious that, in our best sample, the RT recombination band is dominated by the phonon replicas of N–Ga DAP emission, without much additional features. This is opposite to a previous report by Kuwabara *et al.*[17] At 20 K they found a first spectrum (noticed B) similar to the low temperature spectrum observed in this work on sample A. Increasing the temperature, they observed a second spectrum (noticed A) appeared which was attributed to transitions from the conduction band to the Ga acceptors. Such a series of A-B spectra also manifests in Al-doped samples but they are sample dependent and do not resolve systematically.[11] Since in this work we could not observe any "A" band in the entire temperature range investigated, much work is in progress to clarify this point.

VI. CONCLUSION

Ga-acceptor impurities have been introduced in 3C–SiC layers grown on 6H–SiC substrates by the VLS technique. SIMS measurements confirmed a heavy Ga incorporation, with solubility limit close to ~ 3 to 4×10^{19} cm^{-3} when growing in the range of 1050–1300 °C. They revealed also that the *p*-type doping was accompanied by higher N concentration, suggesting *n*-type conductivity. Raman measurements and line-shape fitting of the LO-plasmon coupled mode confirmed that *n*-type conductivity, with electron concentrations in the range of 2×10^{18} cm^{-3} which agrees well with the SIMS results.

At 5 K the LTPL spectra were dominated by strong N–Ga DAP transitions, with usual phonon replicas. In one case the N–Ga DAP features were accompanied by a weaker N–Al DAP ZPL peak, suggesting accidental Ga–Al codoping. From a detailed analysis of the LTPL spectra, the binding energy of Ga and Al acceptors in 3C–SiC (346 meV and 251 meV, respectively) were obtained and the conditions to evaluate optically the [Ga]/[Al] incorporation ratio were discussed. Finally, since the Ga acceptors behave like efficient trapping centers for the photogenerated holes, clear N–Ga DAP spectra could be observed up to 300 K. Similar to N and B codoped 6H–SiC, this suggests possible application as light emitting medium with optical pumping or monolithic light source when combined with nitride based LEDs.

ACKNOWLEDGMENTS

This work was supported in part by the EU in the framework of the MANSiC Project (Grant No. MRTN-CT-2006-035735). Partial support from the French ANR through the Project Blanc-2009 "VHVD" is also greatly acknowledged.

[1]For a recent review, see: *Silicon Carbide: Recent Major Advances*, edited by W. Choyke, H. Matsunami, and G. Pensl (Springer, New York, 2004).
[2]See, for instance: P. Friedrichs, Phys. Status Solidi B **245**, 1232 (2008) and references therein.
[3]A. Schöner, M. Krieger, G. Pensl, M. Abe, and H. Nagasawa, Chem. Vap. Deposition **12**, 523 (2006).
[4]M. Soueidan and G. Ferro, Adv. Funct. Mater. **16**, 975 (2006).
[5]M. Soueidan, G. Ferro, K. Olivier, F. Cauwet, and B. Nsouli, Cryst. Growth Des. **8**, 1044 (2008).
[6]H. Nagasawa, M. Abe, K. Yagi, T. Kawahara, and N. Hatta, Phys. Status Solidi B **245**, 1272 (2008) and references therein.
[7]M. Lazar, C. Jacquier, C. Dubois, C. Raynaud, G. Ferro, D. Planson, P. Brosselard, Y. Monteil, and J. P. Chante, Mater. Sci. Forum **483–485**, 633 (2005).
[8]S. A. Reshanov, I. I. Parfenova, and V. P. Rastegaev, Diamond Relat. Mater. **10**, 1278 (2001).
[9]M. Ikeda, H. Matsunami, and T. Tanaka, Phys. Rev. B **22**, 2842 (1980).
[10]G. Zanmarchi, J. Phys. Chem. Solids **29**, 1727 (1968).
[11]W. J. Choyke and L. Patrick, Phys. Rev. B **2**, 4959 (1970).
[12]J. A. Freitas, Jr., S. G. Bishop, P. E. R. Nordquist, Jr., and M. L. Gipe, Appl. Phys. Lett. **52**, 1695 (1988).
[13]L. L. Clemen, R. P. Devaty, M. F. MacMillan, M. Yoganathan, W. J. Choyke, D. J. Larkin, J. A. Powell, J. A. Edmond, and H. S. Kong, Appl. Phys. Lett. **62**, 2953 (1993).
[14]J. Camassel, S. Juillaguet, M. Zielinski, and C. Balloud, Chem. Vap. Deposition **12**, 549 (2006).
[15]For a review, see: M. Rambach, A. J. Bauer, and H. Ryssel, Phys. Status Solidi B **245**, 1315 (2008).
[16]C.-M. Zetterling and M. Östling, in *Diamond, SiC and Nitride Wide Bandgap Semiconductors*, MRS Symposia Proceedings No. 339, edited by C. H. Carter, Jr., G. Gildenblat, S. Nakamura and R. J. Nemanich, (Materials Research Society, Pittsburgh, 1994), p. 209.
[17]H. Kuwabara, K. Yamanaka, and S. Yamada, Phys. Status Solidi A **37**, K157 (1976).
[18]H. Kuwabara, S. Yamada, and S. Tsunekawa, J. Lumin. **12–13**, 531 (1976).
[19]S. Kamiyama, T. Maeda, Y. Nakamura, M. Iwaya, H. Amano, I. Akasaki, H. Kinoshita, T. Furusho, M. Yoshimoto, T. Kimoto, J. Suda, A. Henry, I. G. Ivanov, J. P. Bergman, B. Monemar, T. Onuma, and S. F. Chichibu, J. Appl. Phys. **99**, 093108 (2006).
[20]T. Troffer, M. Schadt, T. Frank, H. Itoh, G. Pensl, J. Heindl, H. P. Strunk, and M. Maier, Phys. Status Solidi A **162**, 277 (1997).
[21]T. Tsirimpis, M. Krieger, H. B. Weber, and G. Pensl, Mater. Sci. Forum **645–648**, 697 (2010).
[22]Y. A. Vodakov, G. A. Lomakina, E. N. Mokhov, E. I. Radovanova, V. I. Sokolov, M. M. Usmanova, G. F. Yuldashev, and B. B. Machmudov, Phys. Status Solidi A **35**, 37 (1976).
[23]T. Troffer, G. Pensl, A. Schöner, A. Henry, C. Halin, O. Kordina, and E. Jantzen, Mater. Sci. Forum **264–268**, 557 (1998).
[24]M. Gong, S. Fung, C. D. Beling, G. Brauer, H. Wirth, and W. Skorupa, J.

Appl. Phys. **85**, 105 (1999).
[25]A. Henry, C. Hallin, I. G. Ivanov, J. P. Bergman, O. Kordina, U. Lindefelt, and E. Janzén, Phys. Rev. B **53**, 13503 (1996).
[26]C. Jacquier, G. Ferro, M. Zielinski, E. K. Polychroniadis, A. Andreadou, J. Camassel, and Y. Monteil, Phys. Status Solidi C **2**, 1265 (2005).
[27]J. Lorenzzi, G. Zoulis, O. Kim-Hak, N. Jegenyes, D. Carole, F. Cauvet, S. Juillaguet, G. Ferro, and J. Camassel, Mater. Sci. Forum **645–648**, 171 (2010).
[28]S. G. Sridhara, T. J. Eperjesi, R. P. Devaty, and W. J. Choyke, Mater. Sci. Eng., B **61–62**, 229 (1999).
[29]S. Nakashima and H. Harima, Phys. Status Solidi A **162**, 39 (1997).
[30]H. Yugami, S. Nakashima, A. Mitsuishi, A. Uemoto, M. Shigeta, K. Furukawa, A. Suzuki, and S. Nakajima, J. Appl. Phys. **61**, 354 (1987).
[31]M. Grundmann, *The Physics of Semiconductors: An Introduction Including Devices and Nanophysics* (Springer-Verlag, Berlin, Heidelberg, 2006), p. 169.
[32]J. W. Sun, G. Zoulis, J. Lorenzzi, N. Jegenyes, S. Juillaguet, H. Peyre, V. Soulière, G. Ferro, F. Milesi, and J. Camassel, Mater. Sci. Forum **645–648**, 415 (2010).
[33]J. P. Bergman, E. Janzen, and W. J. Choyke, Phys. Status Solidi B **210**, 407 (1998).
[34]L. Latu-Romain, D. Chaussende, C. Balloud, S. Juillaguet, L. Rapenne, E. Pernot, J. Camassel, M. Pons, and R. Madar, Mater. Sci. Forum **527–529**, 99 (2006).
[35]E. Neyret, G. Ferro, S. Juillaguet, J. M. Bluet, C. Jaussaud, and J. Camassel, Mater. Sci. Eng., B **61–62**, 253 (1999).
[36]W. J. Choyke, D. R. Hamilton, and L. Patrick, Phys. Rev. **133**, A1163 (1964).
[37]R. Weingärtner, A. Albrecht, P. J. Wellmann, and A. Winnacker, Mater. Sci. Forum **433–436**, 341 (2003).
[38]M. Lax, Phys. Rev. **119**, 1502 (1960).
[39]D. G. Thomas, M. Gershenzon, and F. A. Trumbore, Phys. Rev. **133**, A269 (1964).
[40]P. J. Dean, E. G. Schonherr, and R. B. Zetterstrom, J. Appl. Phys. **41**, 3475 (1970).